

Laminar to turbulent flow transition in cross-corrugated-plate cavities

Mir-Akbar Hessami, PhD

Department of Mechanical Engineering
Monash University, Clayton, Victoria, Australia 3168

ABSTRACT

It is a common knowledge that the laminar to turbulent flow transition in a pipe or a channel (including cross-corrugated-plate geometries) improves heat transfer and increases pressure loss. Because the two effects are counteractive, it is useful to know when this transition takes place, and what is the magnitude of the improvements so that an optimum flow rate can be selected. Therefore, in this numerical study, the laminar to turbulent flow transition in cross-corrugated channels is investigated using the commercially available CFX-FLOW3D software. The results provided in this paper specify the values of Re_{cr} for flow in such channels with $\beta = 30^\circ, 45^\circ$ and 60° . Also, the results show that while turbulent flow is better for steeper angles of inclination, such a selection for low angles of inclination is not easy to make.

INTRODUCTION

Cross-corrugated parallel plate heat exchangers (CCPPHE's) are used in various process industries because of their compact size and high heat transfer efficiencies. A major disadvantage of these exchangers is their higher pressure loss as a result of the mostly turbulent flow between the plates compared to, for example, shell and tube heat exchangers. While transition from laminar to turbulent flow in a smooth pipe can be expected to occur in the laboratory at around $Re \approx 2300$, such a transition in CCPPHE's can occur at very small flow rates corresponding to Re 's as low as 10, depending on a number of factors the most important of which is the angle of inclination (β) of the corrugation on the plate with respect to the main flow direction (or the axis of the plate). This early transition of flow from laminar to turbulent in these heat exchangers is considered to be responsible for the said high heat transfer and high pressure loss. Therefore, in this paper, the low Re $k-\varepsilon$ turbulent model of the commercially available CFX-FLOW3D software has been used to investigate the characteristics of the fluid flow in the passage between cross-corrugated plates shown in Figure 1, and to determine the critical Reynolds number (Re_{cr}) for flow in such channels for $\beta = 30^\circ, 45^\circ$ and 60° . This information can then be used to optimise the performance of such heat exchangers in terms of the benefits of the high heat transfer and the penalty of the high pressure loss.

A recent review of the literature produced no publication with a focus on the transition from laminar to turbulent flow in cavities typical of CCPPHE's; the

only paper which studied this phenomenon in heat exchangers was that by Esen et al. (1994) [1] for flow in pipes with spirally-shaped roughness. For the flow being studied in this paper, while some researchers do not provide any indication of a transition of the flow regime, other experimental and numerical data reveal specific but differing values of Re_{cr} . For example, the experimental data of Edwards et al. (1984) [2] using APV plates and a number of fluids (including water, oil and glycerol) show a smooth f (Darcy friction factor) vs Re distribution for $1 < Re < 2000$. The experimental work of Luo and Yu (1988) [3] with $\beta = 60^\circ$ and 90° using water provides a fairly constant f value for different flow rates in the range $1000 < Re < 4000$. Similarly, the data published by Okada et al. (1972) [4] do not indicate any change in the slope of f vs Re distribution for a number of plates and β arrangement for $500 < Re < 4000$. Finally, the study by Savostin and Tikhonov (1970) [5] did not report any transition-like behaviour for a number of plate orientations (ie, $\beta = 0^\circ, 10^\circ, 19^\circ, 33^\circ$ and 72°) except for $\beta = 48^\circ$ which showed an increase in the value of f as Re is increased at around $Re \approx 1000$. In contrast, the experimental data of Focke et al. (1985) [6] show a clear transition at $Re_{cr} \approx 8000, 3000, 1800, 400, 500$ and 3000 for $\beta = 0^\circ, 30^\circ, 45^\circ, 60^\circ, 75^\circ$ and 90° , respectively. Similarly, Stasiek et al. (1996) [7] report an apparent transition from laminar to turbulent at $Re_{cr} \approx 2000$ and 1000 for $\beta = 60^\circ$ and 75° respectively. For a non-contacting wavy channel with $\beta = 0^\circ$, Nishimura et al. (1984) [8] report that in the laminar region (ie, $Re < 350$), f is inversely proportional to Re while in the turbulent region they are independent of each other; their experimental data with water and glycerol show this transition clearly.

Although none of these studies concentrates on the transition from laminar to turbulent flow, the latter publications [5-8] rightly indicate that the flow regime passes through a transition, and the value of Re_{cr} is a strong function of β . However, they do not agree with each other on the specific values of Re_{cr} . While the results of the present study verify the presence of a transition from laminar to turbulent flow in the passage between cross-corrugated plates (confirming what should be expected using basic concepts in boundary layer formation, mixing and separation), they also provide detailed information about heat transfer and pressure loss at the transition point. It is shown in this paper that the transition occurs at $Re_{cr} \approx 1100, 2800$ and 3000 for $\beta = 60^\circ, 45^\circ$ and 30° , respectively. Also, the results show the amount of heat transfer and pressure drop enhancement which can be expected as the flow goes from laminar to turbulent regime.

MATHEMATICAL DESCRIPTION AND GEOMETRY OF THE PROBLEM

Plate heat exchangers are constructed by assembling together several pre-fabricated plates, the number of which depends on the intended capacity of the unit. For reasons of heat transfer enhancement, the flow in the channel between the plates is generally perturbed by some form of protrusion on the plate's surface, and the inlet and outlet ports for the hot and cold fluids are arranged in such a way that these fluids flow in opposite directions in the heat exchanger. The flow perturbation in the heat exchangers considered for this study were produced by a wave-like corrugation of known H and P and the corrugation was inclined at an angle β relative to the main flow direction (see Figures 1a and 1b).

The space between two adjacent cross-corrugated plates shown in Figure 1 is comprised of a large number of unit cells (see Figure 2), the corners of which are the contact points between these plates (see Figure 1b). In order to study the flow in such a complex geometry using numerical techniques, a large amount of computer storage and CPU time is needed. However, knowing that the flow in the unit cells far from the edges of the plates, especially near the longitudinal centre of the plates, can be considered to be identical to each other, this geometry is used in the computations reported in this paper. These unit cells can be fully described by specifying H , P and β . For this study, the specific values of these variables were: $P = 25$ mm, $H = 5.5$ mm ($P/H = 4.55$) and $\beta = 30^\circ$, 45° or 60° which were selected so that the results can be compared directly with experimental data of Hessami (1998) [9]; the effects of P/H on heat transfer and pressure drop are given in Hessami (1997) [10].

The numerical results reported herein were generated using the CFX 4.1 (formerly known as CFDS) FLOW3D software purchased from AEA Technology, UK [11]. The geometry and the grid distribution were created by the CFX-MESHBUILD pre-processor, the governing differential equations were solved by CFX-F3D, and the post-processing of the results were done by the CFX-VIEW packages.

The fluid flow and heat transfer in the geometry depicted in Figure 2 can be studied by solving the Navier-Stokes equations presented below (using the summation convention that repeated indices are summed over):

$$\frac{\partial \rho}{\partial t} + \frac{\partial}{\partial x_i} (\rho U_i) = 0$$

$$\frac{\partial \rho U_k}{\partial t} + \frac{\partial}{\partial x_i} (\rho U_i U_k) = -B_k + \frac{\partial \sigma_{ik}}{\partial x_i} \quad \text{where}$$

$$\sigma_{ij} = -p \delta_{ij} + \left(\zeta - \frac{2}{3} \mu \right) \frac{\partial U_k}{\partial x_k} \delta_{ij} + \mu \left(\frac{\partial U_j}{\partial x_i} + \frac{\partial U_i}{\partial x_j} \right)$$

$$\frac{\partial \rho E}{\partial t} + \frac{\partial}{\partial x_i} \left(\rho U_i E - \lambda \frac{\partial T}{\partial x_i} \right) = \frac{\partial p}{\partial t}$$

where E in terms of e is given by $E = e + \frac{\bar{U}^2}{2}$

$$\text{and} \quad \delta_{ij} = \begin{cases} 0 & \text{if } i \neq j \\ 1 & \text{if } i = j \end{cases}$$

In addition to the five equations given above, two other equations were formed by assuming (i) all the flows to be incompressible (a simplified equation of state), and (ii) the fluid specific heat (C_p) to be constant at the specified fluid temperature so that $e = C_p T$ (which is generally known as the constitutive equation). These seven equations were then solved for the seven unknowns, namely, U_i ($i=1,2,3$), p , T , ρ and e .

The numerical results included in this paper were found using a constant heat flux ($q = 1000$ W/m²) wall boundary condition for the top and bottom surfaces of the unit cell shown in Figure 2. The fluid was assumed to enter the unit cell at a given temperature (293 K) through the two inlets I_1 and I_2 with a fully-developed velocity profile (determined by the CFX software) equivalent to the specified mass flow rate. The flow in the cell was assumed to be fully developed, and all fluid properties were allowed to vary with temperature at various grid points in the unit cell.

Taking advantage of CFX's mesh generation capability which can use multi-block structures, the unit cell shown in Figure 2 was formed by two blocks, one for the top and the other for the bottom surfaces of the cell, "glued" together at the interface. However, after some investigations, it became necessary to add additional blocks at the inlet and outlet of each block to smooth-out the flow before it enters the diverging inlets and leaves the converging outlets of the unit cell; without this alteration of the geometry which was originally used by Ciofalo et al. (1996) [12], a stable solution could not be obtained. Therefore, the entire domain was created by joining six body-fitted blocks as shown in Figure 3 in such a way that the space above and below the diamond-shape interface where the top and bottom grooves (each one formed by three blocks) intersect represents the unit cell shown in Figure 2.

The mesh structure in the physical domain is also shown in Figure 3. The mesh and the geometry were generated using CFX MESHBUILD pre-processor. As shown in this diagram, each block is a three dimensional array of differential control volumes over which the governing equations are solved. A fixed number of grid nodes (ie, 22 x 16 x 22) was used for all cases reported herein. Although grid-independence tests were applied on some of the cases studied, no such results are included in this paper. The governing equations given above were solved using the low Re $k-\epsilon$ turbulent flow model; a comparison of this model with laminar and standard $k-\epsilon$ turbulent models, and some experimental data are provided in Hessami (1997) [10].

Mass residual was used as the convergence criterion in this study. All results included herein were computed with a 0.5% mass residual. Mass residual as used in CFX is defined as the error in mass continuity over the entire domain divided by the total mass flow into the unit cell. For all cases, the maximum number of iterations was specified to be 10×10^3 so that the above criterion is always satisfied. The number of iterations taken to obtain a converged solution varied between 200 and 3000 depending on the case being investigated. The corresponding CPU time was in the order of one to 10 hours.

NUMERICAL RESULTS AND DISCUSSIONS

The heat transfer and pressure loss results of the present investigation are plotted in terms of f vs Re in Figures 4a and 4c, and in terms of $Nu/Pr^{0.33}$ vs Re in Figure 4b. The definitions of f , Nu and Re used in this paper are given below:

$$f = \frac{D}{L} \frac{\Delta p}{\rho \bar{U}^2 / 2} \quad Nu = \frac{h D}{k} \quad Re = \frac{\rho \bar{U} D}{\mu}$$

where D is the equivalent diameter of the channel being investigated. Laminar to turbulent flow transition in a smooth pipe is generally characterised by a sharp increase in the value of f when plotted vs increasing Re , and it is known to occur at $Re_{cr} \approx 2300$. Using this criterion, the numerical results provided in Figure 4a clearly show that there is a transition from laminar to turbulent flow at $Re_{cr} \approx 1100, 2800$ and 3000 for $\beta = 60^\circ, 45^\circ$ and 30° , respectively. The sudden increase in pressure loss shown in Figure 4a, is accompanied with similar rise in heat transfer except for $\beta = 30^\circ$ as shown in Figure 4b.

Considering the $\beta = 60^\circ$ case which is the most commonly used angle in commercial heat exchangers, it can be seen from Figures 4a and 4b that both pressure loss and heat transfer increase by a factor of 2-3 as the flow changes from laminar to turbulent. Since the slope of the heat transfer curve is greater in the turbulent region as compared to the laminar region, unlike that for the pressure drop curve which is nearly the same before and after transition, it can be concluded that the heat transfer benefits would outweigh the penalty due to the increase in pressure loss.

In order to check the accuracy of the present numerical data, they are first compared in Figure 4a with $\beta = 60^\circ$ experimental data obtained during this investigation, and other experimental data [3,5] which do not show any transitional behaviour. In Figure 4c, however, published data from the literature [6,8] are used to verify the existence of a transition from laminar to turbulent flow.

Considering the data of Figure 4a, it is clear that the present numerical data especially for $\beta = 60^\circ$ agree fairly well with the present and other published experimental data [3,5]. Knowing that the experimental data refer to a geometry which contains a large number

of unit cells of the type shown in Figure 2, and that the flow in each one of these unit cells may not be fully developed as has been assumed for the numerical study, a difference between the average experimental values and the numerical results can be expected. Although the graphs show that this deviation is not substantial in the range of Re covered by the data, it is difficult to quantify this deviation. The agreement of the present numerical data with experimental data from [6] given in Figure 4c is not as good as that in Figure 4a. It should also be noted that none of the experimental studies has focused on the transition, and hence the lack of sufficiently detailed information to verify the numerical results at the transition point.

The correlation between f and Re in the laminar and turbulent regions for flow in a smooth pipe as reported by Massey (1984) [13] are respectively given by the following equations:

$$f = 64 Re^{-1} \text{ and } f = 0.316 Re^{-1/4} \text{ (Balsius Formula)}$$

Plotting these equations for f vs Re as shown in Figure 4c indicates that the transition takes place at $Re_{cr} \approx 2300$. As mentioned earlier, similar changes in the f vs Re distribution for flow in a wavy channel with $\beta = 0^\circ$ [8] and in cross-corrugated-plate cavities with $\beta = 30^\circ, 45^\circ$ and 60° [6] have been reported in the literature. These results with those found in the present study are also presented in Figure 4c.

The significance of Nishimura's data [8] is in the general trend of the distribution and not in the magnitude of their data because (1) in the laminar region, their data wrongly show a smaller drop in pressure than the smooth pipe, and (2) the transition takes place too early compared to other available data for corrugated channels with $\beta = 0^\circ$. The data reported by Focke et al. [6] show a transition at $Re_{cr} \approx 400, 1800$ and 3000 for $\beta = 60^\circ, 45^\circ$ and 30° , respectively. In contrast, such a transition based on the results of the current study takes place at $Re_{cr} \approx 1100, 2800$ and 3000 as shown in Figures 4a and 4c. It is reasonable to expect Re_{cr} for a cross-corrugated channel to have a value less than that for a smooth pipe; this is not true with the results of Focke et al. for $\beta = 30^\circ$ and the current results with $\beta = 30^\circ$ and 45° . This unexpected finding might be due to the positive effect (ie, delayed transition) which the fluid flow has on the transition in cross-corrugated channels for low values of β similar to the positive influence of riblets on such a transition as reported by Grek et al. (1996) [14]. They have shown that the presence of riblets in a channel has a positive effect on the 3D nonlinear-stage transition structures, and a negative effect on the 2D linear-stage transition structures. Therefore, it is possible that the flow structure in low- β geometries is 3D, and as this angle is further increased the flow structure becomes more two-directional. This speculative explanation obviously needs verification but this is considered to be beyond the scope of this paper.

Careful examination of all the data in Figure 4 shows that

1. for low- β geometries the penalty for high pressure drop is of the same order of magnitude as the gain due to a rise in heat transfer and therefore it is not obvious to recommend the flow to be in the turbulent or laminar regimes, and
2. the slope of the heat transfer curve for $\beta = 60^\circ$ is greater than that for the pressure loss curve in the turbulent region and therefore the improved thermal performance would more than counter-balance the higher cost of pumping.

CONCLUDING REMARKS

The results of a numerical study of fluid flow in a cross-corrugated plate channel reported in this paper show that the laminar to turbulent flow transition takes place at $Re_{cr} \approx 1100, 2800$ and 3000 for $\beta = 60^\circ, 45^\circ$ and 30° , respectively. It is explained that the delayed transition for smaller angles of inclination might be due to the three-dimensional effects of the flow structure. Also, it is shown that turbulent flow is preferable for high- β geometries while such a distinction is difficult to make for low- β situations after comparing the benefits of heat transfer improvements with the penalty of higher pressure losses.

ACKNOWLEDGMENTS

The work reported in this paper was undertaken with financial support from the Australian Research Council and Multistack International Ltd., Boronia, Victoria. Their support has been of great assistance to this study, and is therefore greatly appreciated. Thanks are also due to Mr. V. Alguine for his assistance with the numerical computations reported in this study.

REFERENCES

1. Esen, E. B., Obot, N. T., and Rabas, T. J., **Enhancement: Part I. Heat transfer and pressure drop results for air flow through passages with spirally-shaped roughness**, *Enhancement Heat Transfer*, v 1, n 2, pp 145-156, 1994.
2. Edwards, M. F., Ellis, D. I., and Amooie-Foumeny, M., **The Flow distribution in plate heat exchangers**, *Inst Chem Engineer Symp Series No 86*, pp 1289-1302, 1984.
3. Luo, Di-an and Yu, Yunlin, **Heat transfer, pressure drop and flow visualisation in two corrugated ducts of different corrugation patterns**, *Proc. ASME National Heat Transfer Conference*, Houston, Texas, 24-27 July, 1988, pp 483-488.
4. Okada, K., Ono, M., Tomimura, T., Okuma, T., Konno, H., and Ohtani, S., **Design and heat transfer characteristics of new plate heat exchanger**, *Heat Transfer - Japanese Research*, 1(1), pp 90-95, January-March 1972.
5. Savostin, A. F., and Tikhonov, A. M., **Investigation of the characteristics of plate type heating surfaces** (in Russian), *Teploenergetika*, v 17, n 9, pp 75-78, 1970.
6. Focke, W., Zachariades, J., and Olivier, I., **The effect of the corrugation inclination angle on the thermodynamic performance of plate heat exchangers**, *Int. J. Heat Mass Transfer*, 28(8), pp 1469-1479, 1985.
7. Stasiek, J., Collins, M. W., Ciofalo, M., and Chew, P. E., **Investigation of flow and heat transfer in corrugated passages - I. Experimental results**, *Int. J. Heat Mass Transfer*, 39(1), pp 149-164, 1996.
8. Nishimura, T., Yoshiji, O., and Kawamura, Y., **Flow characteristics in a channel with symmetric wavy wall for steady flow**, *J of Chem Engineering of Japan*, vol 17, No 5, 1984, pp 466-471.
9. Hessami, M. A., **An experimental study of heat transfer in channels formed by cross-corrugated plates**, *Proc. Adelaide Int'l Workshop on Energy Engineering and the Environment*, Australia, 9-10 February, 1998 (in press).
10. Hessami, M. A., **Numerical study of heat transfer and pressure loss in cross-corrugated plate heat exchangers**, *Proc. Third ISHMT/ASME Heat and Mass Transfer Conference*, IIT, Kanpur, India, 29-31 December, 1997, pp 795-802.
11. **CFX 4.1 Flow Solver User Guide**, AEA Technology, Harwell Laboratory, Oxfordshire, United Kingdom, October 1995.
12. Ciofalo, M., Stasiek, J., and Collins, M. W., **Investigation of flow and heat transfer in corrugated passages - II. Numerical simulations**, *Int. J Heat Mass Transfer*, v 39, n 1, pp 165-192, 1996.
13. Massey, B. S., **Mechanics of Fluids**, 5th ed., Van Nostrand Reinhold, Berkshire (UK), 1984, pp 206-215.
14. Grek, G. R., Kozlov, V. V., and Titarenko, S. V., **An experimental study of the effects of riblets on transition**, *J Fluid Mechanics*, v 315, pp 31-49, 1996.

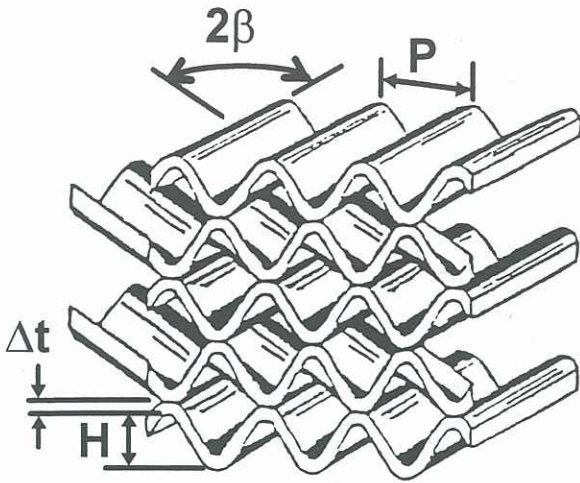


Figure 1a: A close-up view of the cross-corrugation between plates.

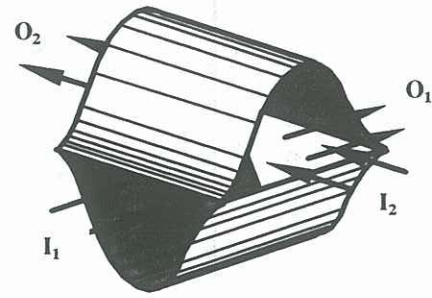


Figure 2: The unit cell structure used in numerical computations.

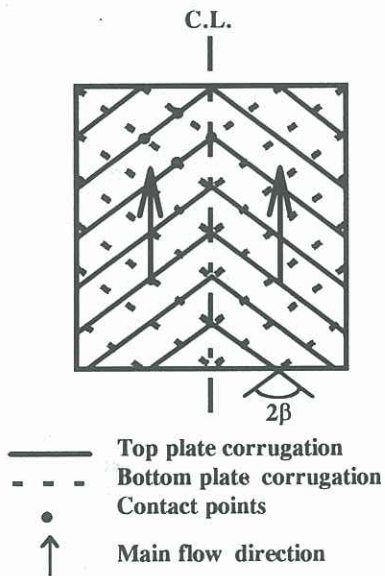


Figure 1b: Flow direction and the corrugation angle.

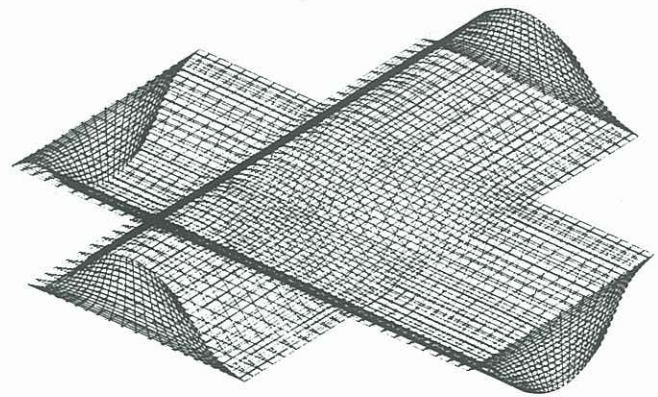


Figure 3: The mesh structure of the geometry used in numerical computations.

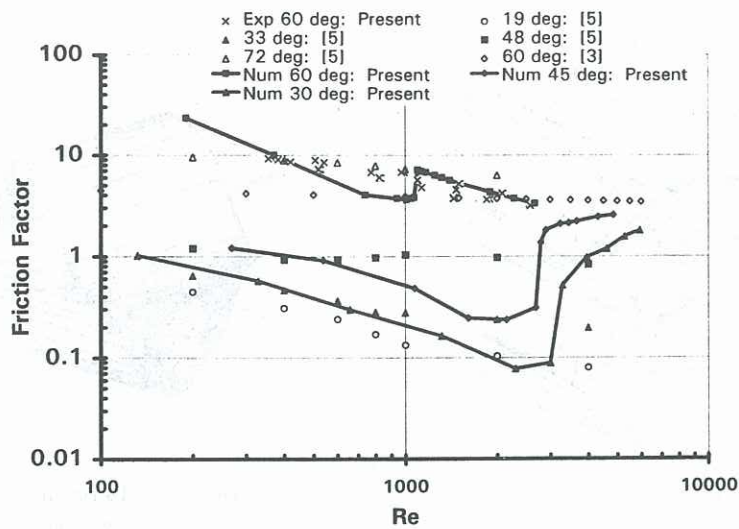


Figure 4a: Comparison of present numerical data with present and published experimental data.

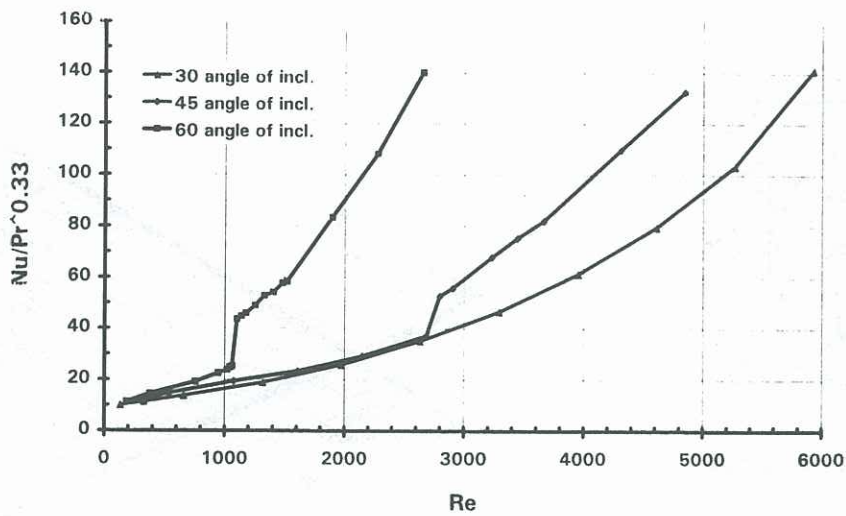


Figure 4b: Effects of varying angle of inclination on heat transfer.

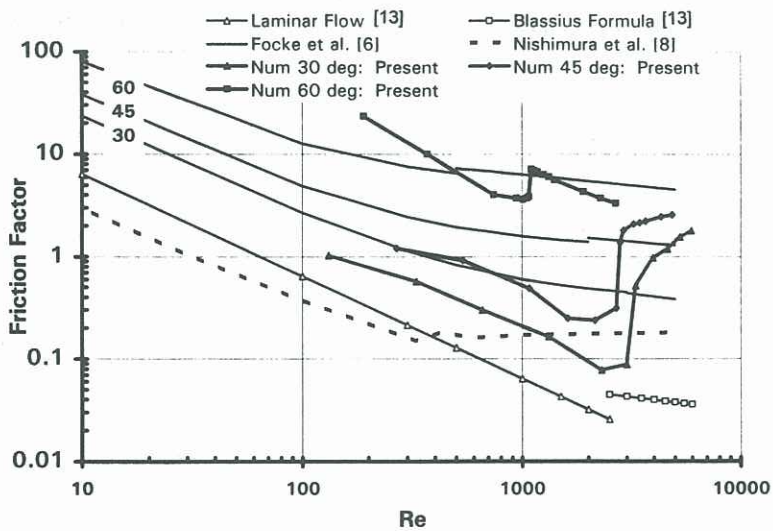


Figure 4c: Comparison of present numerical data with published experimental data .